NUWC-NPT Technical Report 11,571
4 October 2004

Effects of Coupled Biaxial Tension and Shear Stresses on Decrimping Behavior in Pressurized Woven Fabrics

Paul V. Cavallaro
NUWC Division Newport

Ali M. Sadegh
The City College of New York

Claudia J. Quigley
U.S. Army Research, Development & Engineering Command

Arthur R. Johnson
U.S. Army Research Laboratory

NEWPORT

Naval Undersea Warfare Center Division
Newport, Rhode Island

PREFACE

This research was conducted in support of the Center of Excellence for Inflatable Composite Structures at the U.S. Army Natick Soldier Center (NSC) in Natick, MA, through Military Interagency Purchase Request Number 4GS6R00857, NUWC Assignment Number TD0207. The NSC project officer is Jean Hampel.

The technical reviewer for this report was Anthony J. Kalinowski (Code 74).

The authors are especially grateful to Jean Hampel of the NSC for sponsoring this research. Invaluable assistance was received from Federal Fabrics-Fibers Inc. of Lowell, MA, which manufactured the woven air beams and, in particular, from founder Zvi Horovitz and senior engineer Fred Guerts, who participated in informative discussions on the details of the weaving process. Finally, sincere appreciation is extended to Jerry L. Thibodeaux (Code 74) for performing the solids modeling of the test fixture design, to Joseph J. Stace (Code 15232) for conducting the combined biaxial and shear tests, and to both Martin S. Leff (Code 72) and Frank J. Sienkiewicz (Code 72) for performing the strain gauging and calibration operations of fixture's loading plates.

Reviewed and Approved: 4 October 2004

Harriet L. Coleman

Harriet L. Coleman
Head, Ranges, Engineering, and Analysis Department

REPORT DOCUMENTATION PAGE

Form Approved
OMB No. 0704-0188

1. AGENCY USE ONLY *(Leave blank)*	2. REPORT DATE	3. REPORT TYPE AND DATES COVERED
	4 October 2004	

4. TITLE AND SUBTITLE

Effects of Coupled Biaxial Tension and Shear Stresses on Decrimping Behavior in Pressurized Woven Fabrics

5. FUNDING NUMBERS

6. AUTHOR(S)

Paul V. Cavallaro
Ali M. Sadegh
Claudia J. Quigley
Arthur R. Johnson

7. PERFORMING ORGANIZATION NAME(S) AND ADDRESS(ES)

Naval Undersea Warfare Center Division
1176 Howell Street
Newport, RI 02841-1708

8. PERFORMING ORGANIZATION REPORT NUMBER

TR 11,571

9. SPONSORING/MONITORING AGENCY NAME(S) AND ADDRESS(ES)

U.S. Army Research, Development & Engineering Command
Natick Soldier Center
Kansas Street
Natick, MA 01760

10. SPONSORING/MONITORING AGENCY REPORT NUMBER

11. SUPPLEMENTARY NOTES

12a. DISTRIBUTION/AVAILABILITY STATEMENT

Approved for public release; distribution is unlimited.

12b. DISTRIBUTION CODE

13. ABSTRACT (Maximum 200 words)

Tension structures continue to be of increasing importance to military applications requiring both minimum weight, small packing volumes, and enhanced deployment operations. Present design methods for inflated fabric structures, however, are not well established. Analytical tools required to efficiently design these structures lag behind those for conventional structures and materials—partly because of nonlinearities resulting from changes in fabric architecture upon loading. In particular, constitutive relationships must be developed to establish the pressure-dependence and coupling effects of biaxial tension and shear loads. Through analysis and experiment, this study addresses the changes in fabric architecture and, more specifically, the combined effects of biaxial tension, shear, and crimp interchange on the global behavior of woven fabrics. A novel fixture for use in experimental testing of fabrics subjected to combined biaxial tension and shear loads is introduced in this report.

14. SUBJECT TERMS

Inflated Fabric Structures Air Beams Tension Structures Fiber Kinematics Fabric Mechanics Crimp Interchange Finite Element Analysis Weave Braid Biaxial Testing

15. NUMBER OF PAGES
25

16. PRICE CODE

17. SECURITY CLASSIFICATION OF REPORT	18. SECURITY CLASSIFICATION OF THIS PAGE	19. SECURITY CLASSIFICATION OF ABSTRACT	20. LIMITATION OF ABSTRACT
Unclassified	Unclassified	Unclassified	SAR

TABLE OF CONTENTS

LIST OF ILLUSTRATIONS

LIST OF ILLUSTRATIONS (Cont'd)

Figure **Page**

LIST OF TABLES

Table **Page**

EFFECTS OF COUPLED BIAXIAL TENSION AND SHEAR STRESSES ON DECRIMPING BEHAVIOR IN PRESSURIZED WOVEN FABRICS

INTRODUCTION

Tension structures are increasingly important to military applications that require minimum weight, small packing volumes, and enhanced deployment operations. Present design methods for inflated fabric structures, however, are not well established. Analytical tools required to efficiently design these structures lag behind those for conventional structures and materials—partly because of nonlinearities resulting from changes in fabric architecture upon loading. In particular, constitutive relationships must be developed to establish the pressure-dependence and coupling effects of biaxial tension and shear loads. Through analysis and experiment, the research documented in this report addresses the changes in fabric architecture and the combined effects of biaxial tension, shear, and crimp interchange on the global behavior of woven fabrics. Additionally, a novel fixture for use in experimental testing of fabrics subjected to combined biaxial tension and shear loads is introduced.

BACKGROUND

The category of tension structures includes fabric and membrane structures. Both require pre-tensioning loads so that appreciable planar stiffness can be developed. The planar stiffness provides global rigidity, enabling the structure to support both in-plane and lateral loads. Fabric structures utilize a woven or braided construction consisting of discrete tows or yarns that are interlaced with some prescribed level of periodicity. Flexible coatings are primarily applied to the fabric to protect the fibers from sources of environmental degradation; these coatings also may afford some structural rigidity. Membrane structures are constructed using thin films of homogeneous materials and, in general, are isotropic. Multiple films may be bonded together to form a single skin.

Unlike fabric structures, extensive research data are available for membrane structures. Fabric and membrane structures behave fundamentally differently when they are subjected to applied tensile stress fields. The force-displacement response of uncoated fabrics to biaxial tension is dominated by crimp interchange. Crimp is defined as the waviness of a fiber; crimp interchange is the transfer of crimp from one fabric direction to another as a result of loading. Upon initial biaxial loading, tow slippage and rotation occur at the crossover points because inter-tow friction has not yet sufficiently developed. With increasing biaxial tension, crimp interchange along both tow directions occurs and, depending on the ratio of biaxial tensions, crimp may decrease (known as decrimping) or increase. This phenomenon results in a three-dimensional state of deformation that is not present in membrane structures.

The research documented in this report focused on pressurized plain-woven fabric beams in which the source of rigidification may be either air or water. Air-pressurized fabric beams are known as air beams. The plain-woven fabrics considered in this study were constructed from 3000-denier tows rather than yarns. (In general, tows are composed of non-twisted filaments, and yarns are composed of twisted filaments. When compared to denier-equivalent yarns, tows have a greater stiffness but lower strength.) The filaments within the tows were bundled in rectangular-like cross sections to maximize the cover factor by decreasing the fabric crimp heights. A further characteristic pertaining to these tows is that they were formed by layering two 1500-denier tows together using a light coating. This coating served to (1) primarily protect the filaments from environmental effects, (2) contain the filaments in rectangular bundles, (3) enable higher weaving speeds by reducing the friction generated during weaving, and (4) minimize tow compaction during crimp interchange.

Freeston et al.[1] conducted both theoretical and experimental research on the stress-strain behavior of plain-woven fabrics subjected to biaxial loads. Analytic expressions, initially based on Pierce's fabric geometry model for circular yarns,[2] were derived to establish parameters influencing biaxial deformations. The expressions were solved using the nonlinear Newton-Raphson method and were applied to various cases of limiting fabric geometries. A biaxial test fixture was described and used for various ratios of biaxial tension loads. Freeston et al. defined an effective Poisson's ratio (μ_{eff}) as the ratio of lateral contraction of a fill yarn to the extension of a yarn in the warp direction.[1] This parameter captured the three-dimensional nature of fabric deformations, particularly those caused by crimp interchange, for biaxial loads. Their research[1] did not, however, consider shearing loads applied to a biaxially stressed fabric.

Sidhu et al.[3] developed a numerical modeling method coupled with experimental tests to evaluate the performance of composite preforms constructed of plain-woven tows. Their method was based on a unit cell geometry that used a mixture of truss and shell elements. The truss elements explicitly represented the tows with elastic isotropic behavior. The shell elements, which were connected to adjacent tows, provided a fictitious medium through which an *a priori* fabric constitutive behavior could be instituted. Off-axis tensile tests were performed to capture the nonlinear material behavior of the fabric for calibrating the shell elements prior to running the models. While the method did not explicitly compute the tow-to-tow interactions, the effects of those interactions were simulated through the constitutive behavior, as determined by testing.

In contrast, the dominant deformation mode in preform design and drape assessment is fabric shearing (tow scissoring). Here, fabric shearing occurs because the applied tensile stresses are not aligned with the fabric's fiber directions. In the design of plain-woven air beams, however, the biaxial tensile forces resulting from pressurization are aligned with the fabric's nearly orthogonal warp (axial) and weft (hoop) directions. This alignment achieves maximum fabric stiffness. Deformations resulting from pressurization are dominated by inter-tow slippage and crimp interchange rather than tow shearing. Shearing deformations begin to develop, however, when the fabric structure is sufficiently pressurized and external transverse loads are applied.

Motions associated with crimp interchange are kinematic rather than elasticity based and are greater for uncoated fabrics. The effective elastic moduli (E_{warp} and E_{weft}) and in-plane shear

modulus (G_{fab}) of the fabric are nonlinear and highly dependent on the applied biaxial tensile stress. Both experimental[1] and analytical efforts have confirmed that a fabric's force-extension response is initially invariant to the elastic modulus of the tows (E_{tow}). Additionally, G_{fab} was found to be independent of E_{warp}, E_{weft}, and E_{tow}. Likewise, E_{warp} and E_{weft} are independent of E_{tow} for small to moderate biaxial tensions. As the biaxial tension increases, the tows become situated, appreciable friction forces develop, tow compaction occurs, and a decrease in kinematic motions is observed. Appreciable elastic strain energy begins to develop and, upon further tensile loading, the resulting force-extension behavior becomes dependent on E_{tow}.

Hearle et al.[4] identified three distinct regions of stiffness for a uniaxially loaded fabric (see figure 1). Pressurized fabric structures are designed to operate with tow forces ranging between regions I and II to ensure that the tows are loaded well below their breaking strengths, thus providing sufficient factors of safety against burst. When a fabric is biaxially stressed and is then subjected to an in-plane shear stress, the tows will shear and rotate with respect to their original directions.

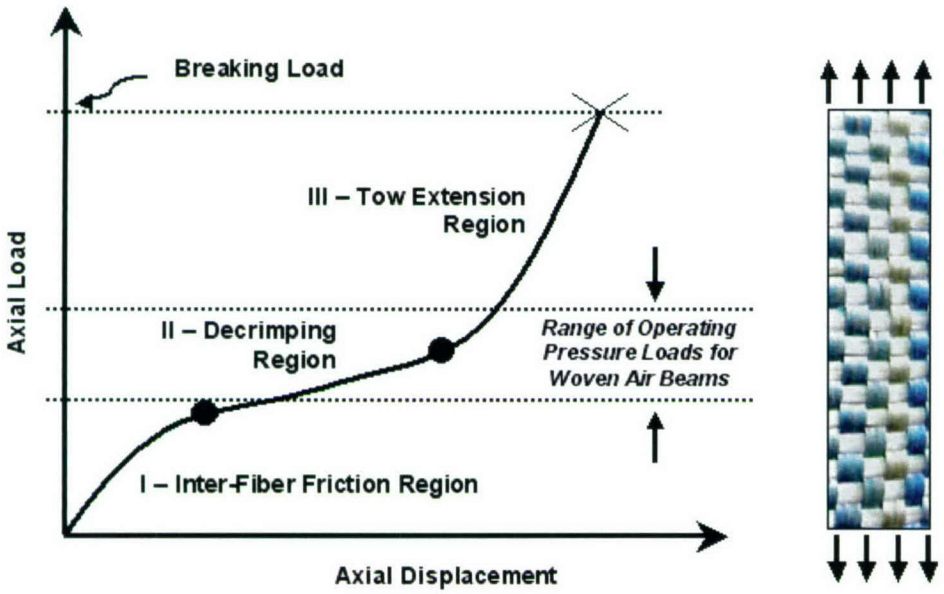

Figure 1. Stages of Axial Stiffness for Woven Fabric Subjected to Uniaxial Tension

The source of initial resistance to shear-induced rotations for an uncoated fabric is the contact-based friction developed at the crossover points. As the shear rotations increase, an upper bound is reached when tows of both directions become kinematically locked. This configuration, shown in figure 2 for pure shear loading, is referred to as "tow jamming." Further shear loading induces localized shear wrinkling instabilities in the fabric, leading to pronounced out-of-plane deformations.

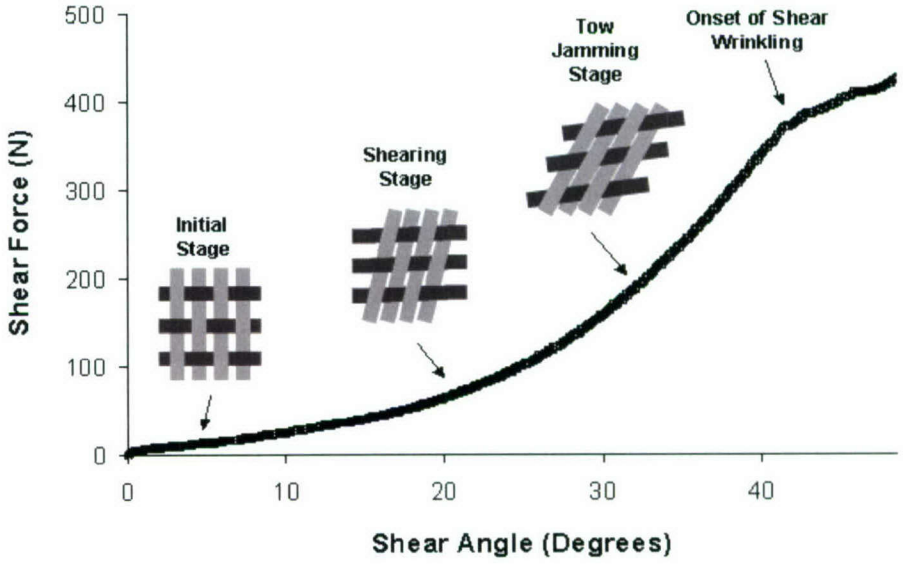

Figure 2. Stages of Shear Stiffness for Pure Shear Loading of a 2:1 Tow Density Ratio (TDR) Woven Fabric

Similar behavior for coated woven fabrics under pure shear loads occurs as described by Farboodmanesh et al.[5] Unlike fabric structures, the homogeneity of membranes excludes the kinematic motions associated with crimp interchange, and strain energy is developed throughout all stages of biaxial tensile loading. Membrane structures, however, are also susceptible to both bending and shear wrinkling instabilities.

Previous analytical and experimental efforts[6, 7] investigated the global flexure response of plain-woven air beams for military shelters (see figures 3 and 4).

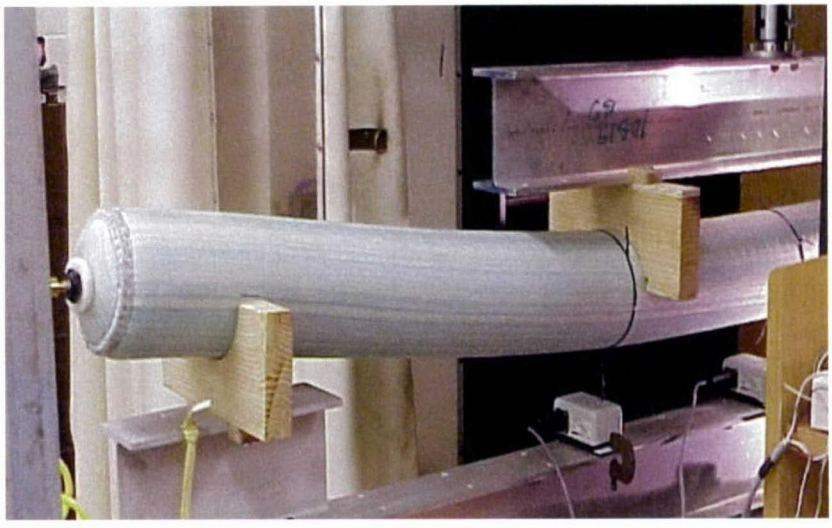

Figure 3. Four-Point Flexure Test of a 15.24-cm-Diameter, Plain-Woven Air Beam Constructed of 3000-Denier, 2:1 TDR Vectran Fabric

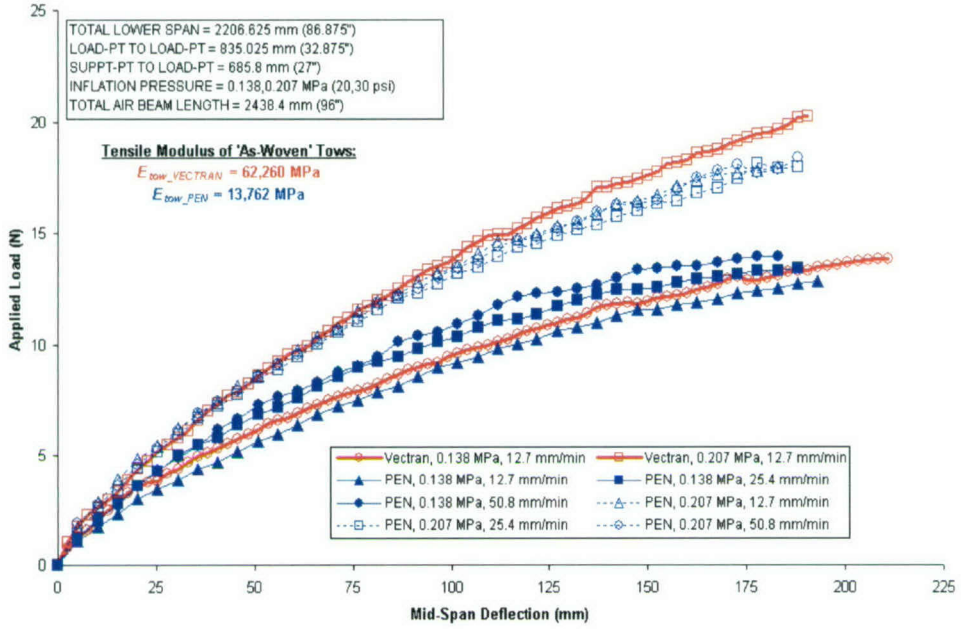

Figure 4. Comparison of 5.08-cm-Diameter Vectran and PEN Air Beams Subjected to Four-Point Flexure Loads

The air beams, constructed of flat tows having zero twist, were inflated to relatively low operating pressures. (Operating pressures are considered to be low when the resulting tow tensions do not exceed 30% of their breaking strength.) In those tests, the flexure behavior of uncoated Vectran and PEN air beams was compared. Both air beams had identical percentage of crimp, TDR, denier, diameter, and length. (TDR is defined as the number of weft (hoop) tows per unit beam length divided by the number of warp (axial) tows per unit circumference.) Although the ratio of the *as-woven* moduli of the Vectran and PEN tows obtained through tow tensile tests was 4.7 to 1.0, there were minimal differences in deflections of the beams at a given inflation pressure. It was observed that the global bending behavior of the air beams was (1) invariant with E_{tow} for the range of inflation pressures considered, (2) dominated by the kinematics of crimp interchange and (3) subjected to considerable transverse shearing deformations. The effects of crimp interchange and shearing deformations preclude the use of traditional strength-of-materials design methods for plain-woven fabric air beams.

FINITE ELEMENT MODELING

This research focused on plain-woven fabric air beams. Air beams are routinely made using a 2:1 TDR to ensure equi-biaxial loading of the tows during inflation; such loading provides identical factors of safety against burst in the warp and weft tow directions. In contrast with conventional structures, E_{warp}, E_{weft}, and G_{fab} for inflatable fabric structures are nonlinear and highly dependent on inflation pressure, fabric construction, TDR, and even the applied loads.

Localized models of the interacting tows were developed using homogenization techniques to capture the effects of crimp interchange on the force-extension response of the fabric and to predict global fabric moduli. The models, developed using the ABAQUS[8] finite element program, are shown in figures 5 and 6.

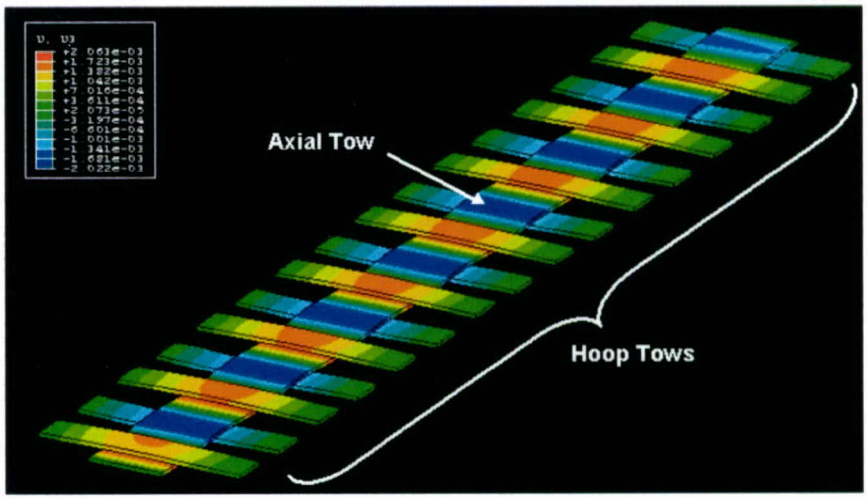

Figure 5. Localized Finite Element Model of a 2:1 TDR Fabric Strip Subjected to Biaxial Tension (Out-of-Plane Displacements Shown)

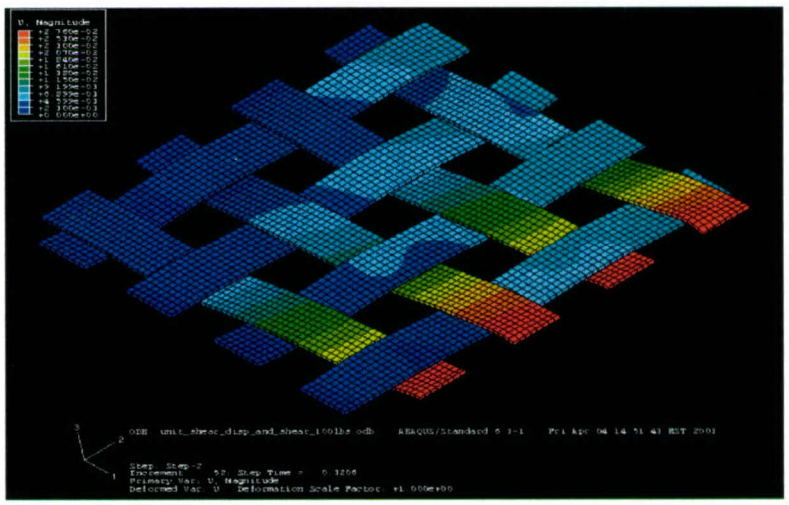

Figure 6. Localized Unit Cell Finite Element Model of a 2:1 TDR Fabric Subjected to Combined Biaxial Tension and In-Plane Shear

The models were formulated to capture the nonlinear deformation modes attributed to possible tow-to-tow contact interactions associated with crimp interchange and shearing. These modes included tow slippage, scissoring, extension, bending, compaction, and inter-tow friction. The crimp interchange effects were sources of substantial nonlinearities as shown in the global elastic and shear moduli predictions in figures 7 and 8 for uncoated plain-woven fabrics.

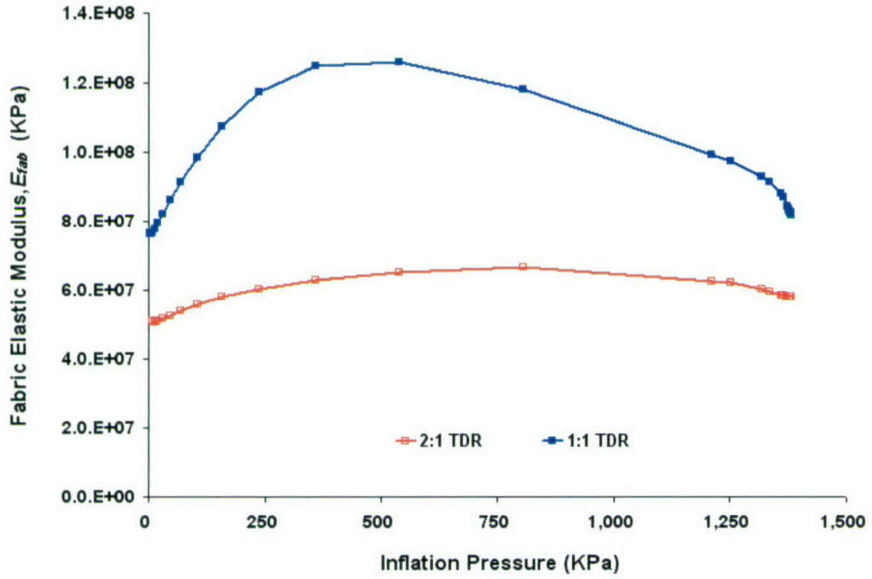

Figure 7. Fabric Elastic Modulus (E_{fab}) Versus Inflation Pressure as Predicted by the Fabric Strip Model

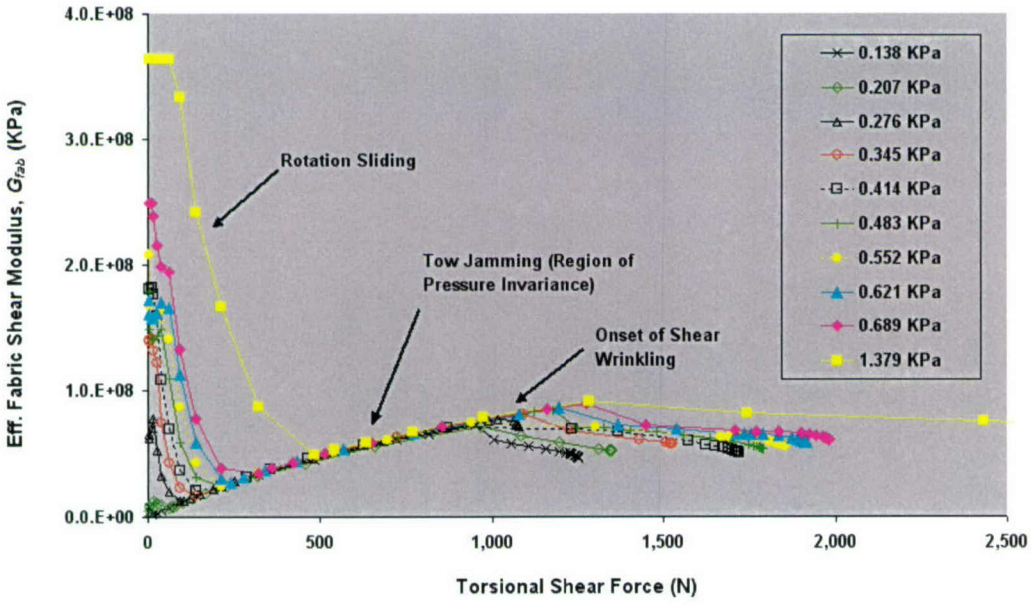

Figure 8. Fabric Shear Modulus (G_{fab}) Predictions as Functions of Inflation Pressure and Shear Force for a 2:1 TDR Plain-Woven Fabric

During crimp interchange, the contact areas at the crossover points changed with increasing loads. Localized plots of the hoop and axial tows taken from the fabric strip model during crimp interchange showed the presence of cupping and doubly-curved surface deformations. The contact areas were highly non-uniform—not unexpected because the filaments, and subsequently the tows, have a non-zero bending stiffness (EI), creating a radius of curvature in the tows at the crossover points. As the biaxial loads increased, the radius of curvature in the tows increased and the tows attempted to achieve a nearly flat configuration. The contact forces, however, were distributed locally on the four corners of the crossover regions.

EXPERIMENTAL FIXTURE

A combined multi-axial tension and shear test fixture[9] was recently designed and manufactured to permit simultaneous measuring of E_{warp}, E_{weft}, and G_{fab} for structural fabrics. The fixture (see figure 9) was designed for use with conventional tension/torsion machines to characterize the elastic and shear moduli of fabrics. The test fixture, which uses a cruciform-shaped specimen, evaluates both strength and stiffness properties of various fabric architectures such as weaves, braids, and knits. For fabrics constructed of two principal fiber directions, the fixture uses two rhombus-shaped frames connected with rotary joints (see figure 9).

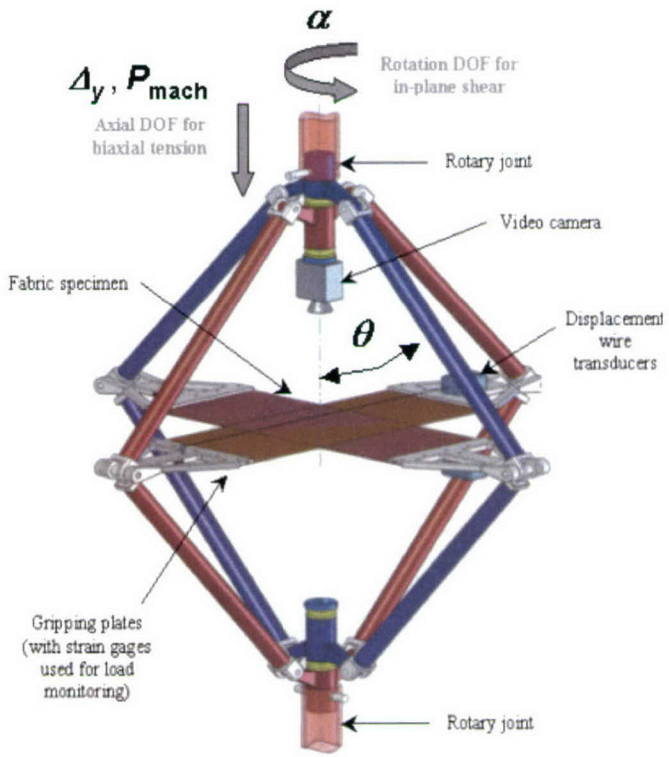

Figure 9. Combined Biaxial Tension and In-Plane Shear Fixture with Axial and Rotational Degrees of Freedom

Assuming that the lower joint assembly is pinned to a stationary crosshead of the test machine, the relationship between the downward vertical displacement of the upper joint (Δ_y) and the equi-biaxial extension (Δ_{ext}) exerted on the fabric is given by

$$\Delta_{ext} = 2\left[\sqrt{L^2 - \left[L^2\cos^2\theta - L\Delta_y\cos\theta + \left(\frac{\Delta_y}{2}\right)^2\right]} - L\sin\theta\right], \tag{1}$$

where θ = the initial angle of the upper tube from vertical reference, and L = the length of the upper tube (pin-to-pin).

Similarly, the relationship between the machine-applied vertical force (P_{mach}) and the forces along each fabric direction (F_{warp} and F_{weft}) is given by

$$P_{mach} = \frac{F_{warp} + F_{weft}}{\tan\left(\theta + \frac{\Delta_{ext}}{2L}\right)}. \tag{2}$$

To simulate the stress state caused by inflation of woven air beams, a biaxial load was computed based on the air beam diameter, operating pressure, and TDR. Biaxial loading begins by moving the crosshead of the test machine in a downward vertical motion so that the machine applies a vertical load (P_{mach}) to the fixture. Doing so creates an equal extension (Δ_{ext}) along both tow directions, resulting in biaxial tensile loads F_{warp} and F_{weft} as shown in figure 10.

Figure 10. Biaxial Tension Mode

Strain gauges mounted on the loading plates used in conjunction with load-versus-strain calibration curves provide the tensile force measurements along the warp and weft directions. Once the biaxial extension is applied to the specimen, a torsional load is then superimposed to induce relative rotation between the tow directions, creating an in-plane shearing as shown in figure 11.

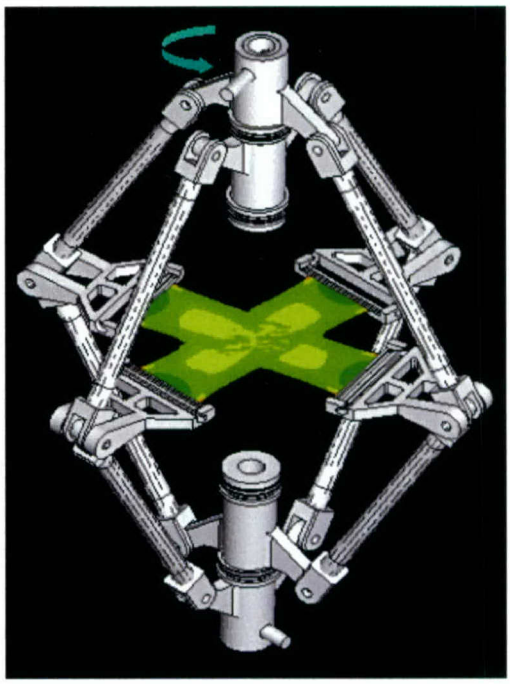

Figure 11. In-Plane Shear Mode

EXPERIMENTAL RESULTS

Fabric specimens constructed of 3000-denier dimensionally stable polymer (DSP) tows with a 1:1 TDR and 13 tows per inch along both the warp and weft directions were tested under combined biaxial and shear loadings. The specimens were carefully cut so that tows along each direction ran continuously between loading plates. Figure 12 shows the time-history inputs from the test machine and the corresponding loading responses of a specimen. The three distinct loading phases shown in figure 12 were identified as the biaxial loading phase (I), the combined biaxial and shear loading phase (II), and the biaxial loading with shear unloading phase (III). The test machine was operated in a load-controlled (rather than displacement-controlled) mode so that, upon reaching a specific machine load (P_{mach}), the feedback/control loop continuously adjusted the crosshead displacement to keep the biaxial loads nearly constant during phases II and III.

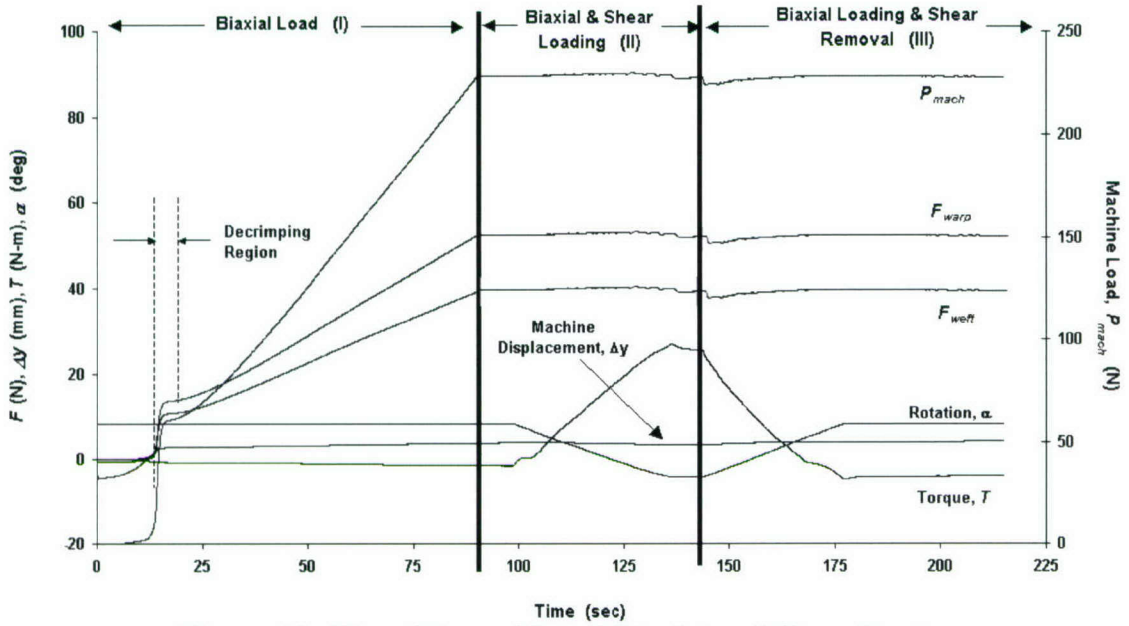

Figure 12. Time-History Plot of Biaxial and Shear Testing of 3000-Denier, 1:1 TDR DSP Fabric

A machine load P_{mach} of 4448 N was applied during the biaxial loading of phase I, resulting in warp and weft direction forces of 1032 N and 742.9 N, respectively. Figure 13 shows the force-versus-extension behavior for the DSP fabric during the biaxial loading of phase I only.

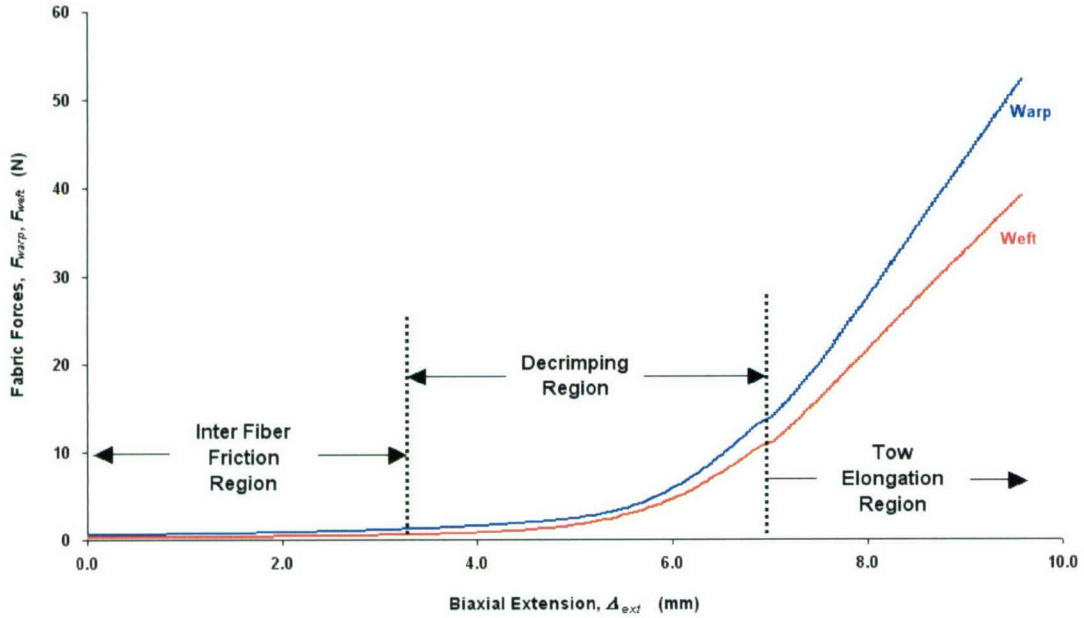

Figure 13. Fabric Forces F_{warp} and F_{weft} Versus Δ_{ext} for 3000-Denier, 1:1 TDR Plain-Woven DSP Fabric

Three distinct regions were recognized during phase I and were similar to those identified by Hearle et al.[4] (see figure 1) for uniaxial loads. During the inter-fiber friction region, the filaments within the tows, as well as the tows themselves, became aligned with the directions of loading. Minimal resistance to the biaxial extension was developed. When the inter-tow frictional forces were exceeded, tow slippage—which led directly to the decrimping region—was initiated. At the onset of decrimping, relative motions among crossover points achieved their peaks. Upon further extension, relative tow motions decreased, crimp heights decreased at the crossover regions, and significant resistance to extension developed. At the end of the decrimping region, the tows became situated, leading to the tow-elongation region. In the tow-elongation region, no kinematic motions were observed and appreciable strain energy developed within the tows. In summary, the inter-fiber friction and tow-elongation regions were observed to be nearly linear. The decrimping region, which represented a transition region where fabric stiffnesses developed, was, however, highly nonlinear.

The imbalance of fabric forces observed during phase I for the 1:1 TDR plain-woven DSP fabric was attributed to unequal crimping along the warp and weft directions. Crimp is defined as the percentage difference between a tow's straightened length (after it is removed from the weave and subjected to a nominal force) and its original as-woven length. A particular source of crimp imbalance for 1:1 TDR fabrics is uneven tow tensions during the weaving process. The consequence of crimp imbalance is unequal fabric stiffnesses in the warp and weft directions. When a crimp-imbalanced fabric is subjected to equi-extensional loading, the resulting reaction forces produced in the warp and weft tows will be unequal. Physical measurements of the DSP fabric revealed an average crimp ratio ξ of 0.76 as defined by equation (3):

$$\xi = \frac{C_{weft}}{C_{warp}}, \tag{3}$$

where C_{weft} = % crimp along the weft direction and C_{warp} = % crimp along the warp direction. Crimp results of three tows measured in each direction are summarized in table 1.

Table 1. Crimp Measurements for 3000-Denier, 1:1 TDR Plain-Woven DSP Fabric

Tow Axis	Tow Spec. #	Woven Ref. Length (mm)	Tow Length (mm)	ΔL (mm)	C (%)
Warp	1	257.18	261.94	4.76	1.85
Warp	2	257.18	261.94	4.76	1.85
Warp	3	257.18	261.94	4.76	1.85
				Average C_{warp} =	1.85
Weft	1	260.35	266.70	6.35	2.44
Weft	2	260.35	266.70	6.35	2.44
Weft	3	260.35	266.70	6.35	2.44
				Average C_{weft} =	2.44
				C_{warp} / C_{weft} Ratio, ξ =	0.76

A cursory observation suggests that the ratio of the warp-to-weft direction forces (F_{warp}/F_{weft}) is a function of ξ for equi-extension loadings; that is,

$$\frac{F_{warp}}{F_{weft}} = f(\xi). \tag{4}$$

Generation of engineering stress-strain curves from the force-extension data was relatively simple. First, to compute the warp (σ_{warp}) and weft (σ_{weft}) stress, the total cross-sectional areas of all tows (A_{tows}) in each direction had to be identified in accordance with the denier-related properties of the tows shown in table 2; that is,

$$A_{tows} = \pi \frac{d_{fil}^2}{4} N_g N_{fil}, \tag{5}$$

where d_{fil} is filament diameter, N_{fil} is the number of filaments in tow, and N_g is the number of tows gripped.

Table 2. Denier-Related Properties for DSP Tows

	DSP
Tow Denier	3000
No. Filaments, N_{fil}	546
Filament Diameter, d_{fil} (cm)	0.00241
Tow Area (cm^2)	0.00250

It then follows that

$$\sigma_{warp} = \frac{F_{warp}}{A_{tows}}, \tag{6a}$$

and

$$\sigma_{weft} = \frac{F_{weft}}{A_{tows}}. \tag{6b}$$

The engineering strains along the warp and weft directions (ε_{warp} and ε_{weft}, respectively) were equal because both directions were subjected to equal extension amounts and possessed the same grip lengths (L_g); therefore, the engineering strain (ε) is given by

$$\varepsilon = \varepsilon_{warp} = \varepsilon_{weft} = \frac{\Delta_{ext}}{L_g}. \tag{7}$$

Figure 14 plots the stress-strain curves along the warp and weft tow directions. As expected, the stress-strain curves were similar in shape to the force-extension curves. The fabric elastic moduli developed along the warp and weft directions (E_{warp} and E_{weft}, respectively) were computed as the ratios of stress to strain. Figure 15 plots curves of the developed elastic moduli versus the force in the corresponding directions. The elastic moduli were significantly nonlinear and unequal because of the crimp imbalance of the DSP fabric.

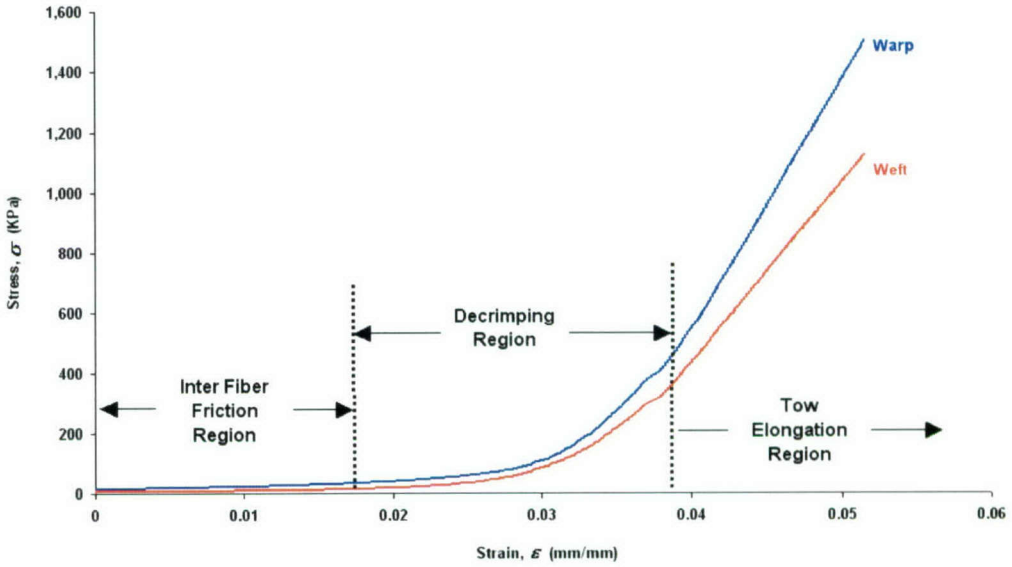

Figure 14. Stress-Strain (σ-ε) Curves for 3000-Denier, 1:1 TDR Plain-Woven DSP Fabric Subjected to Biaxial Extension

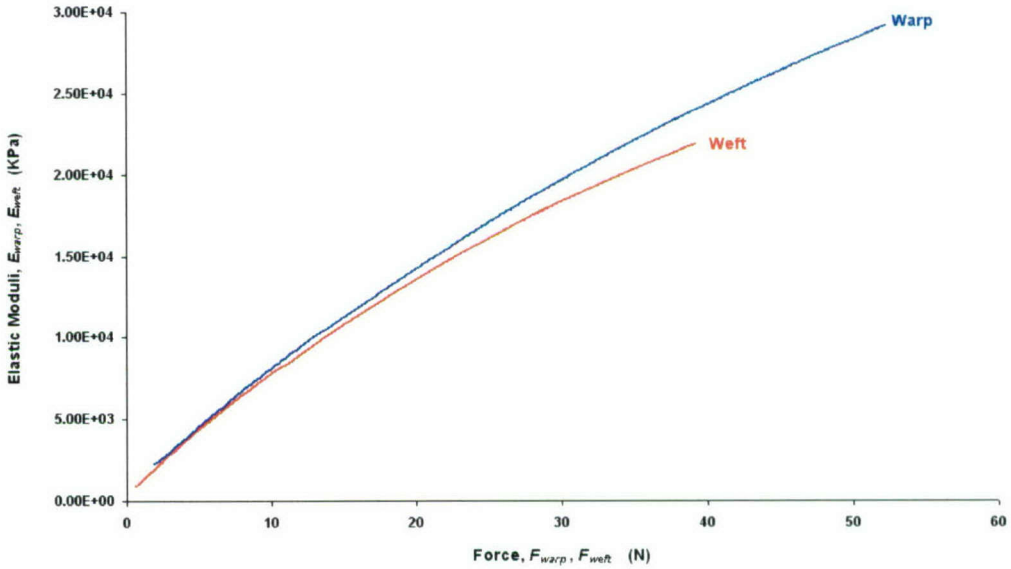

Figure 15. E Versus F Along Warp and Weft Directions for 3000-Denier, 1:1 TDR Plain-Woven DSP Fabric Subjected to Biaxial Extension

In phase II (see figure 12), combined biaxial and shear loading began. Relative rotation between the warp and weft directions was initiated, and the corresponding torque (T) generated by the specimen was recorded. During this phase, the use of load-controlled testing was particularly important. As the rotation (α) between tow directions developed, additional crimp interchange occurred, altering the original tow tensions developed in phase I. To maintain constant biaxial loads, the test machine automatically adjusted the crosshead displacement to compensate for changes in biaxial tension (see figure 16).

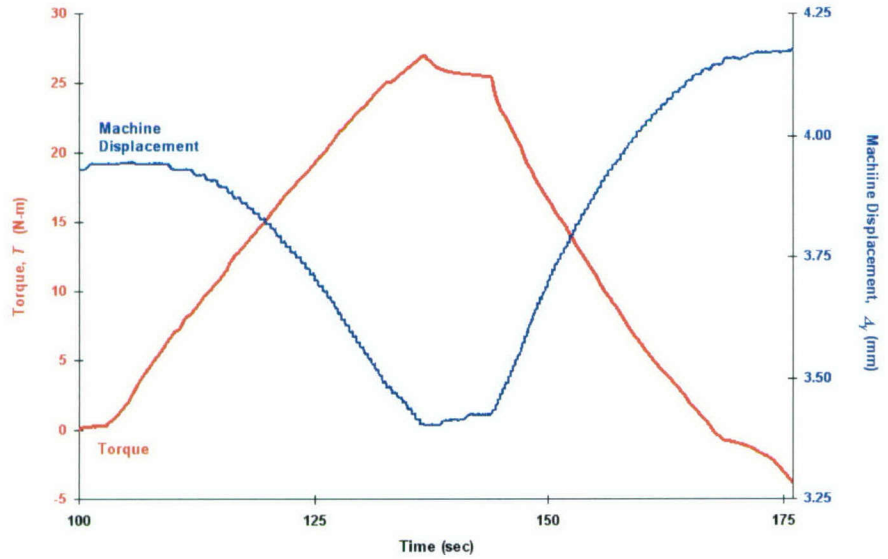

Figure 16. Time-History Plot of T and Δ_y for 3000-Denier, 1:1 TDR Plain-Woven DSP Fabric During Phases II and III

Figure 17 shows the T versus α response of the DSP specimen to phases II and III for three levels of biaxial tension. The rotational resistance, measured as torque, increased substantially with increasing biaxial tension. The initial portions of the curves shown in figure 17 include transition regions, after which the torque resistance becomes fully developed. The intermediate regions indicate the presence of a dwell where the applied torque remains constant with increasing rotation. The dwell is caused by rotational sliding of the orthogonal tows at the crossover points. Note that, upon return to the initial zero-rotation reference, a negative torque was required. Although hysteresis was observed, it was attributed to architectural changes in the fabric. Specifically, the filaments and tows were unable to return to their exact original positions prior to rotation. Such changes were considered kinematic in nature rather than strain energy based.

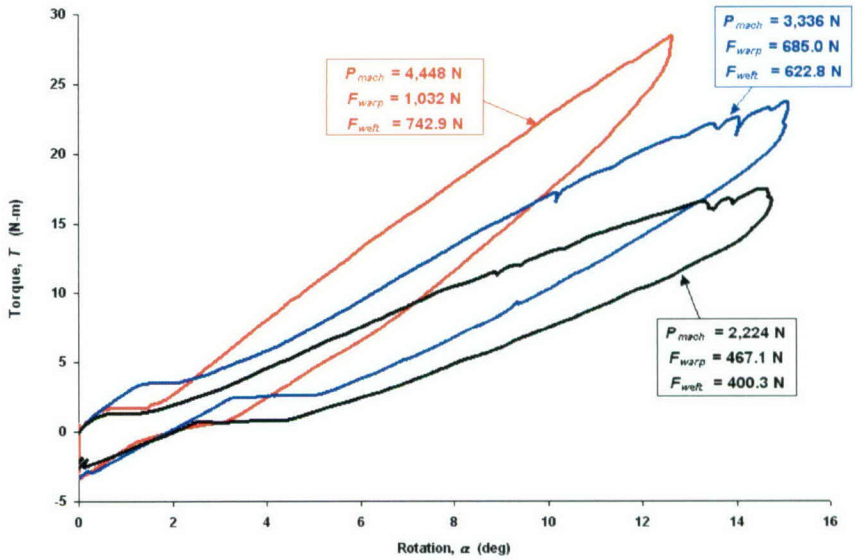

Figure 17. T Versus α Response During Phases II and III for a 3000-Denier, 1:1 TDR Plain-Woven DSP Fabric Subjected to Various Biaxial Tensions

The fabric shear stress (τ) was computed from the torque (T) and the separation distance between opposing grips (d_g) by the following equation:

$$\tau = \frac{T}{d_g A_{tows}}. \tag{8}$$

The fabric shear strain (γ) was equal to the rotation angle (α) expressed in units of radians. Figure 18 plots the shear stress versus shear strain response for three levels of biaxial tension. These curves are similar in shape to the T-α curves.

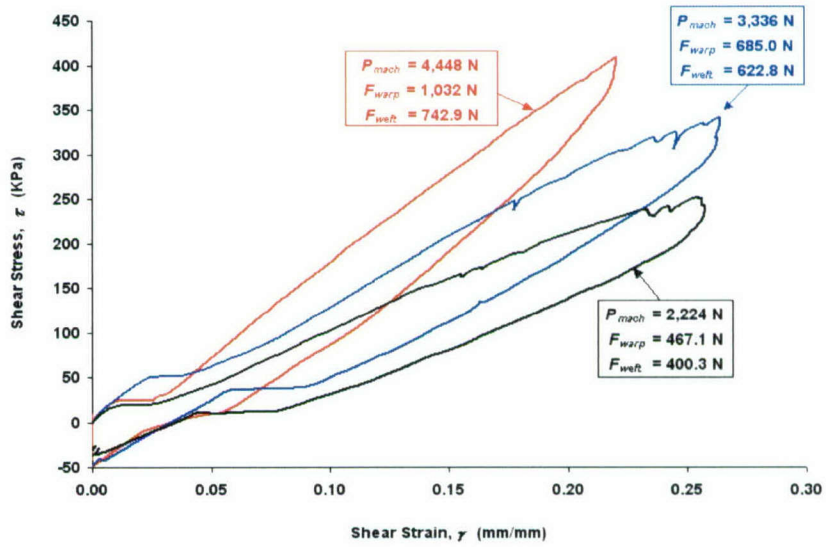

Figure 18. τ Versus γ Response During Phases II and III for a 3000-Denier, 1:1 TDR Plain-Woven DSP Fabric Subjected to Various Biaxial Tensions

The fabric shear modulus (G_{fab}), obtained by dividing τ by γ, is plotted in figure 19 as a function of α for three levels of biaxial tension.

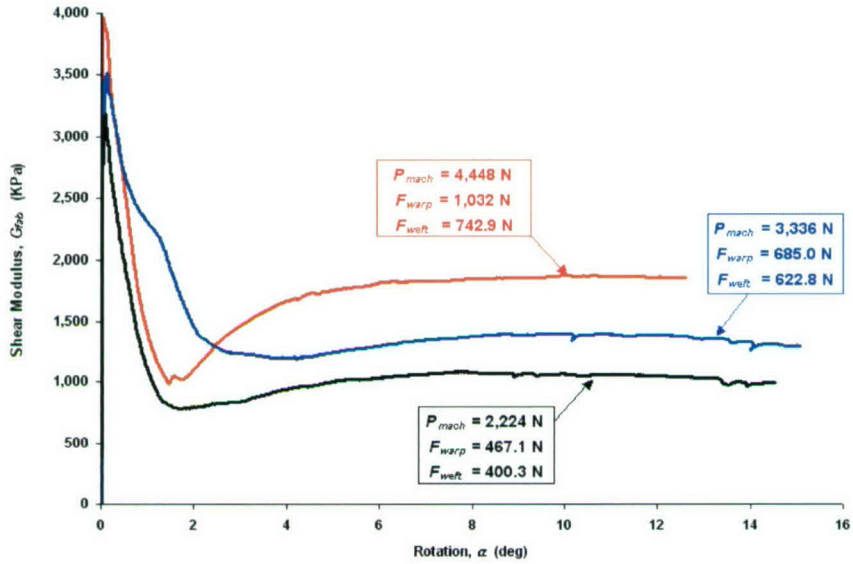

Figure 19. G_{fab} Versus α Response During Phases II and III for a 3000-Denier, 1:1 TDR Plain-Woven DSP Fabric Subjected to Various Biaxial Tensions

The shear modulus increased proportionally with increasing biaxial tensions. Relative peak values of G_{fab} occurred at initially small rotations prior to the onset of rotational slip between orthogonal tows. When the frictional resistance at the crossover points was exceeded, the rotational slip was met with minimal resistance. Further rotation resulted in crimp interchange that exceeded what was generated in phase I and acted as a stiffening mechanism. Relative plateaus in shear stiffness were then observed prior to the onset of tow jamming. The "slip/stick" phenomena observed during loading phases II and III were dominant sources of nonlinearities in figures 17 through 19.

This study also evaluated the performance of the test fixture and cruciform-shaped specimens and found that, although the test fixture performed successfully, improvements could be made in the specimen shape to minimize end effects. In general, common problems for cruciform-shaped fabric specimens, regardless of the type of test fixture used, arise from end effects caused by loading differences among the tails and central region. For example, during biaxial extension, the tails were subject to uniaxial loads; at the same time, the central region was undergoing biaxial loading. Within the tail regions, tows perpendicular to the extension direction remained unloaded. No resistance to the decrimping of the loaded tows was provided. Because crimp interchange and the resulting extension were dependent on the loading ratio between fabric directions, the cruciform specimen provided lower bounds of both elastic and shear moduli; therefore, cruciform specimens should be sized for minimum tail dimensions to the most practical extent permissible. In the limiting case, however, where the tail length approaches zero, the rotation angle available from the present fixture for shear loading also approaches zero. This effect is due to interference among adjacent loading plates.

CONCLUSIONS

The fundamental difference between membrane and fabric materials is that fabric materials are subjected to architectural changes in microstructure when mechanical loads are imposed on them—specifically at the tow and filament levels. These changes profoundly influence the load-carrying capability of woven fabrics. Three distinct regions of stiffness—similar to a woven fabric's uniaxial behavior—were revealed for biaxial loadings. Of particular importance was the decrimping region in which crimp interchange was initiated, dramatic reductions in crimp heights occurred, and appreciable elastic and shear stiffnesses developed. It is through these architectural changes that woven fabrics become suitable for use in structural applications; however, because the mechanisms associated with decrimping are highly nonlinear and the biaxial tension and shear behavior are coupled, suitable design methods for woven fabric structures are not yet established.

The present analyses and experiments represent methods for establishing the coupled elastic and shear moduli of woven fabrics, as well as for evaluating the performance of pressurized air beam structures. Each method requires a thorough assessment of the construction details at the fabric, tow, and filament levels. As did Freeston et al.,[1] this research found that visual inspections were insufficient for determining if the fabric specimens were initially square (symmetric in terms of tow counts, spacings, directional uniformity, etc.).

Crimp measurements were necessary to identify any imbalances that impacted the decrimping response and the subsequent load-extension behaviors. A potential cause of crimp imbalance for 1:1 TDR fabrics was identified as unequal tensions in the warp and weft directions during the weaving process. It is recommended that fabric test specimens be preconditioned with repeated biaxial loadings at a nominal level—a process that, in this research, reduced the variations in crimp uniformity along each tow direction of the tested specimens. In general, these variations resulted from specimen handling and, once the variations were minimized, greater uniformity, repeatability, and convergence of crimp measurements and load ratios were achieved.

Because the analyses were conducted prior to the development of the biaxial test fixture, the models did not accurately reflect the exact construction details of the tested specimens; therefore, a complete correlation could not be pursued. Qualitative comparisons, however, show agreement on the decrimping and coupled biaxial tension/shear effects.

While it is generally recognized that structural fabric applications may be categorized as residing in the extension (strain) domain or the force domain, the need to characterize fabric mechanical properties in both domains exists; therefore, design modifications are underway to enable the fixture to optionally provide equi-biaxial loadings. Future efforts will address the optimization of the cruciform-shaped specimen to alleviate end effects and the testing of a variety of fabric materials constructed with various TDRs and coatings.

REFERENCES

1. W. D. Freeston, M. M. Platt, and M. M. Schoppee, "Mechanics of Elastic Performance of Textile Materials, Part XVIII, Stress-Strain Response of Fabrics Under Two-Dimensional Loading," *Textile Research Journal*, vol. 37, 1967, pp. 948-975.

2. F. T. Pierce, "The Geometry of Cloth Structure," *Journal of the Textile Institute*, vol. 28, no. 3, 1937, pp. T45-T96.

3. R. M. J. S. Sidhu, R. C. Averill, M. Riaz, and F. Pourboghart, "Finite Element Analysis of Textile Composite Preform Stamping," *Journal of Composite Structures*, vol. 52, 2001, pp. 483-497.

4. J.W.S. Hearle, P. Grosberg, and S. Backer, *Structural Mechanics of Fibers, Yarns and Fabrics*, John Wiley & Sons Inc., New York, 1969.

5. S. Farboodmanesh et al., "Effect of Construction on Mechanical Behavior of Fabric Reinforced Rubber," *Rubber Division Meeting*, American Chemical Society, Pittsburgh, PA, 8-11 October 2002.

6. P. Cavallaro, A. Sadegh, and M. Johnson, "Mechanics of Plain-Woven Fabrics for Inflated Structures," *Journal of Composite Structures*, vol. 61, no. 4, 2003, pp. 375-393.

7. C. Quigley, P. Cavallaro, A. Johnson, and A. Sadegh, "Advances in Fabric and Structural Analyses of Pressure Inflated Structures," *Conference Proceedings of the 2003 ASME International Mechanical Engineering Congress and Exposition*, IMECE2003-55060, November 2003.

8. *ABAQUS Version 6.3*, 2003, ABAQUS Inc., Pawtucket, RI.

9. P. Cavallaro, A. Sadegh, and C. Quigley, "Combined In-Plane Shear and Multi-Axial Tension or Compression Testing Apparatus," Patent Application, Navy Case # 84916, Naval Undersea Warfare Center Division, Newport, RI, April 2004.

INITIAL DISTRIBUTION LIST

Addressee	No. of Copies
Office of Naval Research (ONR-334 (R. Barsoum))	1
U.S. Army Natick Soldier Center (AMSRD-NSC-CP-CE (S-145): C. Quigley, F. Kostka, J. Hampel, K. Santee, K. Horak; AMSSB-RCP-C: M. Jee, J. Roche, J. Cullinane; AMSSB-RAD-D(N): G. Thibault, R. Benny, J. Miletti, G. Gildea; T. Godfrey; M. Roylance)	14
Northeastern University (J. N. Rossettos)	1
Army Research Laboratory Analytical & Computational Methods Branch (ACMB (3), MS-240 (A. R. Johnson))	4
Army Research Laboratory Weapons and Materials Research Directorate (AMSRL-WM-MB (R. Dooley, D. Granville))	2
Federal Fabrics-Fibers Inc. (Z. Horovitz, F. Guerts)	2
Vertigo Inc. (G. Brown)	1
U.S. Army Engineer Research and Development Center, Coastal and Hydraulics Laboratory (D. Resio, J. Melby, J. Fowler)	3
U.S. Army Research Office (A. Rajendran, G. Anderson, B. LaMattina)	3
The City College of New York (A. Sadegh)	5
Defense Technical Information Center	2
Center for Naval Analyses	1